PHYSICAL REVIEW B VOLUME 25, NUMBER 4 15 FEBRUARY 1982

Electronic theory of ordering and segregation in binary alloys: Application to simple metals

Mark O. Robbins and L. M. Falicov
Department of Physics, University of California, Berkeley, California 94720
(Received 24 July 1981)

An electronic theory for the total energy of binary alloys is developed and applied successfully to alkali-alkali— and noble-noble—metal alloys. The theory uses the extended cluster-Bethe-lattice method to compute the electronic density of states. A new scheme for incorporating the long-range effects of the Coulomb interaction is developed and used to determine the parameters of the Hamiltonian self-consistently as a function of the charge transfer between the elemental components. This approach allows the energy of a binary alloy to be calculated as a function of arbitrary concentration and short-range order with the use of only properties of the pure constituents.

I. INTRODUCTION

There has been considerable interest[1–5] in the systematics of the heats of formation (ΔH_F) of metallic alloys recently. However, ΔH_F is only a single aspect of a broader problem, the dependence of an alloy's free energy on the positional correlations between the different types of atoms within it. This dependence is central to the study of order-disorder transitions[6] and even to the interpretation of experimental values for ΔH_F. In this paper we investigate a model which allows the electronic energy of an alloy to be calculated over the entire range of concentration and positional correlations. The method is not *ab initio,* but requires only information about the pure elemental constituents of the alloy. Information about the stoichiometric AB compound is useful, if available, but not necessary. This input information is readily calculated using standard band-structure techniques which cannot be directly applied to alloys. As a test we apply the model to alloys of simple metals.

Almost all theoretical treatments of positional correlations concentrate on one of two limiting types: short-range order (SRO), which describes correlations over the range of a few atomic spacings, or long-range order (LRO), which describes the large-distance limit of the correlations. In this paper we study the effect of SRO on the electronic energy of an alloy, specifically the effect of correlations between nearest-neighbor sites. The implications for LRO can be derived trivially if the constituent atoms tend to segregate, but are somewhat more complicated if they prefer to form a compound. The configurational entropy of the alloy can be found using Kikuchi's cluster-variation method[7] and combined with the electronic energy to predict phase diagrams for the alloy. However, in this paper we consider only the energy, leaving detailed description of thermal effects to a later date.

Many methods of calculating the electronic density of states of alloys have been developed.[8–16] However, only a few, the recursion method,[13] cluster coherent-potential approximation (CPA),[14] and cluster-Bethe-lattice method (CBLM),[15,16] can include both the effects of short-range order and of charge transfer. Charge transfer is important because the degree of SRO affects both the amount of charge transfer and its effect on the self-consistent one-electron Hamiltonian of the alloy. As we show later, the alloy's energy is affected significantly by charge transfer.

All the methods mentioned above are based on the same physical picture. The self-consistent one-electron Hamiltonian and SRO are treated exactly within a cluster of atoms, and the remainder of the alloy is replaced by an effective medium. The projected local density of states (LDOS) on the central site of the cluster is assumed to be relatively insensitive to the approximations made outside the cluster. It can be integrated to find the charge transfer and electronic energy of the alloy. This information can then be used to determine new parameters for the one-electron Hamiltonian and, if feasible, the process can be iterated to self-consistency.

The major differences between the competing methods are in computational difficulty and in the properties of the effective medium. Little progress has been made in using the cluster CPA to incorporate SRO in actual calculations. The recursion method may include SRO in an effective medium, but not in a transparent fashion. Calculations are made for larger and larger clusters and extrapolated to produce the effective medium. One cannot study the properties of the effective medium independently, and computation is difficult because large clusters must be treated exactly before the extrapolation is made.

We work with an extension[16] of the CBLM. The effective medium has the same SRO and coordination number as the alloy, but has the geometry of a Cayley tree (or Bethe lattice).[17] This is a topological construction equivalent to a network without closed rings of bonds. The LDOS of the Cayley tree effective medium can be evaluated independently and, for a single band, only involves the solution of a quartic equation.

The formalism we use is very similar to that of Kittler and Falicov.[16] The main difference is in the treatment of interatomic Coulomb interactions arising from charge transfer. We include the long-range nature of the Coulomb interaction so that the model can be consistently applied to the entire possible range of concentration and SRO.

Section II contains a description of the model with emphasis on the treatment of the interatomic Coulomb interaction. Section III presents the results of the model for binary alloys of monovalent metals and compares them to the experimentally observed properties of simple-metal alloys. Section IV gives a summary and conclusions.

II. MODEL

A. SRO parameters

The SRO parameters which are incorporated in the effective medium are the pair probabilities. A bond in a binary alloy of A and B atoms can have four configurations: $A-A$, $A-B$, $B-A$, and $B-B$. The fraction of bonds of type $(I-J)$ is denoted by y_{IJ}. Symmetry requires that $y_{AB}=y_{BA}$, and normalization requires

$$\sum_{IJ} y_{IJ}=1 . \tag{1}$$

Thus there are only two independent-order parameters. It is most convenient to choose these to be $x=c_A$, the concentration of A atoms, and σ, a variable describing the degree of correlation in the occupation of neighboring sites.[18] In terms of x and σ the concentrations and pair probabilities are

$$\begin{aligned} &c_A=x, \quad c_B=1-x , \\ &y_{AA}=x^2+x(1-x)\sigma , \\ &y_{BB}=(1-x)^2+x(1-x)\sigma , \\ &y_{AB}=y_{BA}=x(1-x)(1-\sigma) . \end{aligned} \tag{2}$$

Note that when $\sigma=0$ neighboring sites are not correlated, i.e., the pair probabilities are just the product of the relevant concentrations. For $\sigma>0$ an atom is more likely to be surrounded by atoms of the same type, and for $\sigma<0$ it is more likely to be surrounded by atoms of the opposite type.

In Fig. 1 we show the parameter space defined by x and σ. Three limiting types of SRO are identified. For $\sigma=1$, the alloy is *segregated,* there are no $A-B$ or $B-A$ bonds. When $\sigma=0$ the distribution of atoms in the alloy is *random,* $y_{IJ}=c_I c_J$. A *binary-ordered* arrangement is one in which either y_{AA} or y_{BB} is zero. Atoms are surrounded by unlike atoms to the maximum possible degree. For structures with only even-numbered rings, the value of σ in the binary-ordered limit is

$$\begin{aligned} &\sigma=-x/(1-x), \quad x\le\tfrac{1}{2} \\ &\sigma=-(1-x)/x, \quad x\ge\tfrac{1}{2} . \end{aligned} \tag{3}$$

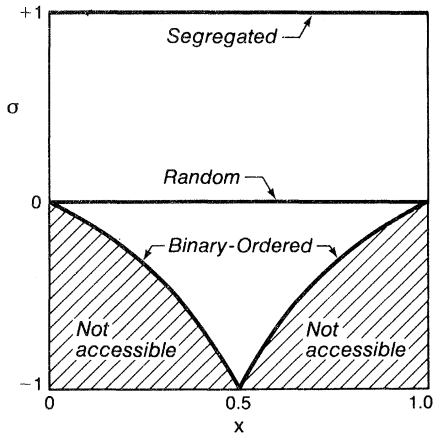

FIG. 1. Accessible region in the (x,σ) parameter space. Lines of segregated, random, and binary-ordered configurations are shown.

B. Extended CBLM

A complete discussion of the extended CBLM is presented in Ref. 16. What follows is a brief review of the method.

The starting point for the theory is a tight-binding Hartree Hamiltonian with nearest-neighbor hopping only. It is convenient to work in real space because the alloy has no translational symmetry, because SRO parameters only describe the immediate environment of an atom, and because the Coulomb energy from charge transfer is easily calculated. In this section we assume that the effective one-electron parameters of the Hamiltonian are known. The following section describes the self-consistent inclusion of Coulomb interactions.

The general form for the Hamiltonian is

$$H=\sum_{i\mu}E_{i\mu}n_{i\mu}+\sum_{i\mu,j\nu}t_{i\mu,j\nu}a^{\dagger}_{i\mu}a_{j\nu}-\tfrac{1}{2}H_{ee}\ , \qquad (4)$$

where i and μ indicate the site and type of an orbital; $a^{\dagger}_{i\mu}$, $a_{i\mu}$, and $n_{i\mu}$ are creation, annihilation, and number operators for the given orbital; $E_{i\mu}$ and $t_{i\mu,j\nu}$ are the on-site and hopping matrix elements of the Hamiltonian. The site index i determines the type of atom at the site. Half of the electron-electron interaction, H_{ee}, must be subtracted because it is double-counted in the effective one-electron Hamiltonian. The hopping elements $t_{i\mu,j\nu}$ are assumed to vanish unless i and j are nearest neighbors. For convenience the local basis is chosen so that the on-site elements

$$E_{i\mu,i\nu}=E_{i\mu}\delta_{\mu\nu}\ . \qquad (5)$$

The local density of states $D_{i\mu}(E)$ of an orbital μ at site i is related to the diagonal element of the Green's function:

$$D_{i\mu}(E)=-\pi^{-1}\mathrm{Im}[G_{i\mu,i\mu}(E)]\ ,$$

where

$$G_{i\mu,j\nu}(E)=\langle i\mu\,|\,\hat{G}(E)\,|\,j\nu\rangle\ . \qquad (6)$$

The equations for $G_{i\mu,i\mu}(E)$ couple it to all other sites through the hopping elements of the Hamiltonian. Dyson's equation gives

$$\begin{aligned} EG_{i\mu,i\mu}&=1+E_{i\mu}G_{i\mu,i\mu}+\sum_{j\nu}t_{i\mu,j\nu}G_{j\nu,i\mu}\ ,\\ EG_{j\nu,i\mu}&=E_{j\nu}G_{j\nu,i\mu}+\sum_{\substack{k\neq i\\ \lambda}}t_{j\nu,k\lambda}G_{k\lambda,i\mu}\\ &\quad+t_{j\nu,i\mu}G_{i\mu,i\mu}\ ,\\ &\text{etc.} \end{aligned} \qquad (7)$$

The quantity of interest is the ensemble average of the LDOS taken over all states of the alloy consistent with the assumed SRO. It is not possible to solve Eqs. (7) for all arrangements of 10^{23} atoms and then perform the ensemble average. The first approximation of the extended CBLM is to take the ensemble average in the equations determining G rather than averaging G itself. This is equivalent to replacing the actual local environment of each atom with an effective environment determined self-consistently by the pair probabilities.

The second approximation of the extended CBLM is the Bethe-lattice approximation. The real lattice is replaced by a Bethe lattice which has the same coordination number, but contains no rings of bonds. This simplifies the equation for the matrix $G_{j\nu,i\mu}$.

The effective medium models the local environment of an atom very well. The coordination number and distribution of nearest-neighbor pairs are reproduced exactly. Longer-range fluctuations in the local environment and the influence of rings of bonds can only be included in the cluster of atoms, which is treated exactly. However, Falicov and Yndurain[15] have investigated the effect of rings of bonds and find that the LDOS remains qualitatively the same.

We are interested in the total energy and charge transfer, which are integrated properties of the LDOS. Previous research[19] suggests that such properties are much less sensitive to approximations than specific details of the LDOS itself. The effect of approximations is also reduced because we are only interested in the *change* in energy with short-range order. Absolute errors in the calculated total energy cancel. It is thus reasonable to expect the extended CBLM to give an accurate description of the dependence of an alloy's energy on SRO.

C. Interatomic Coulomb interactions

The LDOS calculated for given parameters of the one-electron Hamiltonian can be integrated to find the mean charge on A and B atoms. Charge conservation dictates that

$$c_A\Delta_A+c_B\Delta_B=0\ , \qquad (8)$$

where Δ_I is the mean difference in the number of electrons around a type-I atom from the atomic value. The distribution of charges produces a Coulomb potential which must be incorporated

into the one-electron Hamiltonian, leading to new values for the charge transfer, etc. At each step the Coulomb potential falls off as r^{-1} even if the alloy is metallic. Screening is the result of the approach to self-consistency. It cannot occur at any individual step because the charge distribution is fixed by the one-electron Hamiltonian.

If a complete set of local orbitals is used the Coulomb potential is $q/\epsilon_0 r$, where ϵ_0 is the vacuum dielectric constant. Practical calculations must be limited to orbitals with energies near the fermi energy. One can approximate the effect of other orbitals by using a different value for ϵ. The screening process is thus treated on two levels. The redistribution of electrons within orbitals on the same site is treated approximately through ϵ, and the charge transfer between sites is treated explicitly and self-consistently. In what follows we assume ϵ does not vary significantly with SRO and treat it as a phenomenological parameter. If the ratios of the atomic polarizabilities to atomic volumes of the alloy's constituents are very different, this may not be a good assumption.

Our objective is to find a reasonable interpolation scheme for the mean effect of the Coulomb potential on the Hartree parameters of the Hamiltonian. Previous treatments have only considered the effect of a finite cluster on the Coulomb potential at a site.[16,20] This is a bad approximation for alloys near the limits of segregating or binary order because the Coulomb potential is long range. Any charge transfer between macroscopic regions of segregated atoms produces an infinite potential and no finite cluster can reproduce this. In a binary-ordered compound, the Coulomb potential from other atoms is proportional to the Madelung constant which is also a long-range property of the system. The potential from a finite cluster is only a good approximation to the total potential near the random limit. In this regime the charge distribution averages to zero within a few atomic spacings.

The parameters of the Hartree Hamiltonian that are most affected by the long-range character of the Coulomb potential are the on-site energies. The hopping matrix elements are mainly determined by the local environment. Self-consistent changes in these parameters may be incorporated using conventional methods.

To find the change in on-site energies we calculate the mean distribution of types of atoms around a given atom and sum the interatomic Coulomb interaction over all sites. The alloy is assumed to have only substitutional disorder, i.e., the distribution of types of atom is disordered but all atoms are located on a regular periodic lattice. We also assume that each atom can be assigned its mean charge transfer and that the charge is reasonably localized and spherically distributed.[21] The average Coulomb potential $\bar{\phi}_I$ on a type-I atom due to atoms at all other sites $\vec{R}_l$ is then

$$\bar{\phi}_I = \sum_{\vec{R}_l \neq 0} V\left(\frac{R}{|\vec{R}_l|}\right) \sum_J g_{IJ}(\vec{R}_l)\Delta_J \ , \tag{9}$$

where R is the nearest-neighbor separation, $V = e^2/\epsilon R$ is the nearest-neighbor contribution per electron transferred, and $g_{IJ}(\vec{R}_l)$ is a correlation function giving the probability of finding a type-J atom at a position $\vec{R}_l$ relative to a type-I-atom.

The correlation function must be consistent with the pair probabilities, but cannot be uniquely determined from them.[22] However, an approximate form for $g_{IJ}(\vec{R}_l)$ can be derived which is exact in the random and segregated limits for all concentrations and in the binary-ordered limit for the stoichiometric AB compound. The approximation amounts to ignoring higher-order positional correlations which are consistently left out of the theory. The correlation function is assumed to depend only on n, the smallest number of nearest-neighbor bonds connecting $\vec{R}_l$ to the origin. The pair probabilities are then used[23] to define a recursion relation for $g_{IJ}(n)$:

$$g_{IJ}(n+1) = \sum_K g_{IK}(n)\frac{y_{JK}}{c_K} \ . \tag{10}$$

One finds

$$\bar{\phi}_I = V\Delta_I \alpha(\sigma) \ , \tag{11}$$

where $\alpha(\sigma)$ is a simple function with no concentration dependence. The details of the calculation are given in the Appendix.

Figure 2 shows $\alpha(\sigma)$ for a bcc lattice. Note that it has the correct behavior in the three limits of SRO. For $\sigma \to -1$, $\alpha(\sigma)$ approaches the Madelung constant; for $\sigma \to +1$, $\alpha(\sigma)$ becomes infinite; and $\alpha(0) = 0$. The derivative at $\sigma = 0$ is also correct. Near random SRO only the first shell has an appreciable mean charge. The magnitude of the charge on each atom of the first shell is $\sigma\Delta_I e$, and thus

$$\alpha(\sigma) \simeq Z\sigma \ , \tag{12}$$

where Z is the number of nearest neighbors. If we only considered the potential from nearest neigh-

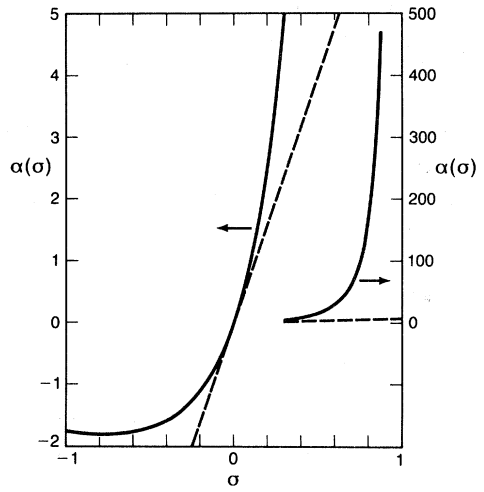

FIG. 2. Coefficient $\alpha(\sigma)$ of the interatomic Coulomb sum as a function of short-range order σ.

bors,[16] this form for α would hold for all σ. It is clear from Fig. 2 that this is not a good approximation for $|\sigma| \gtrsim 0.1$.

For intermediate values of σ there may be further corrections to α, because of higher-order positional correlations. Changes in α of a few percent do not appreciably affect our results.

D. Application to monovalent metals

To study the predictions of the extended CBLM, we consider the simplest case, alloys of atoms with one valence electron each. A single s-like orbital is used as the basis on each site and the cluster is taken to be of one atom. The on-site Coulomb interaction is treated in the mean-field approximation. Its strength U_i may depend on the type of atom at the site. Spin ordering is not considered.

The Hamiltonian becomes

$$H = \sum_{is} E_i n_{is} + \sum_{ijs} t_{ij} a_{is}^{\dagger} a_{js} - \tfrac{1}{2} H_{ee} \ , \tag{13}$$

where s indicates the spin index, and where the self-consistent on-site energy E_i and the on-site energy without charge transfer E_{i0} are related by

$$E_i = E_{i0} + \left[\sum_s n_{is} - 1 \right] \left[\tfrac{1}{2} U_i + V\alpha(\sigma) \right] . \tag{14}$$

The electron-electron interaction is

$$H_{ee} = \sum_{is} (E_i - E_{i0}) n_{is} \ . \tag{15}$$

The on-site and hopping parameters are assumed to depend only on the types of atoms on the relevant sites.[24] An arbitrary alloy is then specified by its lattice, seven energy parameters ($C = E_{B0} - E_{A0}$, t_{AA}, t_{AB}, t_{BB}, U_A, U_B, and V), and two order parameters (x and σ). The energy parameters can all be derived from properties of the elemental constituents using the prescriptions discussed below.

We have estimated energy parameters for alkali-alkali— and noble-noble—metal alloys (Table I).[25] The on-site energy difference C was taken to be the difference in the ionization potentials[26] of the constituent atoms. The pure, elemental hopping

TABLE I. Energy parameters.

Element	W (eV)	t_{II} (eV)	E_{I0}[a] (eV)
Li	11.22[b]	1.060	−5.390
Na	7.79[b]	0.736	−5.138
K	3.96[b]	0.374	−4.339
Rb	3.28[b]	0.310	−4.176
Cs	2.31[b]	0.218	−3.893
Cu	15.57[c]	1.471	−7.724
Ag	13.39[d]	1.265	−7.574
Au	14.42[e]	1.363	−9.220

[a]Reference 26.
[b]Reference 27.
[c]Reference 28.
[d]Reference 29.
[e]Reference 30.

parameters t_{II} were fitted to band-structure calculations.[27–30] The band structures for the alkali metals are clearly not fitted well by a single tight-binding band. An approximate bandwidth was defined by taking the difference in energies of the lowest states of even symmetry under inversion at the center (Γ_1) and corner (H_{12}) of the bcc Brillioun zone, $W=E(H_{12})-E(\Gamma_1)$. The value of t_{II} was then determined by requiring that the CBLM produce the same bandwidth,

$$t_{II}=W/4\sqrt{7}=W/4\sqrt{Z-1}\ .$$

In lithium the first band is actually narrower than W because a p-like state, at the H corner, H_{15}, has lower energy. The hopping parameters for the noble metals were determined in the same way, using the energy difference between the Γ_1 and W_3 states of the fcc Brillouin zone to define the bandwidth.

Our model for the interatomic Coulomb interaction does not apply to an fcc lattice because it has odd-numbered rings of bonds. We cannot apply our technique at arbitrary SRO, but we can compare the results in the random and binary-ordered limits where $\alpha(\sigma)$ is zero and equal to the Madelung constant, respectively. A fact related to the odd-numbered rings is that no structure with $\sigma=-1$ is possible. The ordered configuration adopted by CuAu is $L\,1_0$ and has alternate layers of like atoms stacked along the [100] direction.[6,31] The distribution of nearest-neighbor pairs is consistent with $\sigma=-\frac{1}{3}$. We take this value as the SRO at $x=0.5$ in the binary-ordered limit in calculating properties of noble-noble–metal alloys. The energy gained from hybridization is probably underestimated because there is no special long-range order in the Bethe-lattice effective medium at $\sigma=-\frac{1}{3}$.

In the absence of calculations on the binary-ordered compounds and for the Coulomb coefficients we used two prescriptions to determine energy parameters. A variety of physical models suggest that t_{AB} should be close to the geometric mean t of the pure elemental t_{II}. Rough calculations based on both free-electron and Hückel-type models for alloys of simple metals gave values for t_{AB}/t which range from 0.9 to 1. Values less than 1 are associated with sizable differences in the atomic radii.

The only remaining free parameters are U_A, U_B, and V. For most purposes we choose $U_A=U_B$. Ferromagnetic instabilities occur for U larger than $\frac{1}{3}$ of the bandwidth. We use a value near this limit in calculations for real systems.

The relative magnitudes of U and V are obtained by means of a scheme suggested by Rudnick and Stern.[20] In this scheme the distribution of charge on the shell of nearest neighbors is assumed to be approximately spherical. The ratio U/V is then determined by requiring the potential due to a uniform charge on the shell to be the same on the central site and on the nearest neighbors. For a bcc lattice this gives $U/V=6.422$. For an fcc lattice $U/V=7.552$.

A better prescription for the on-site Coulomb repulsion may be to make U_I inversely proportional to the atomic radii. This choice improves the quantitative agreement between model and experiment for all the alloys we consider, but the effects are not substantial.

Size effects are known to play an important role in determining the stable configuration of an alloy. In our model we have chosen parameters which are essentially suited for alloys of equal-sized elements. Size differences introduce complications of various types: changes in the hopping parameters, local elastic distortions, and inhomogeneities of the diagonal and off-diagonal elements of the Hamiltonian. We have not included these effects here because they introduce much too many uncontrollable parameters. We have explored, however, the effects of size difference in the specific alloys described below and we have found that no qualitative changes are produced. The most important qualitative feature associated with size differences is the empirically established fact[6] that size differences of more than 15% lead, in general, to the absence of continuous-solid solutions. However, it is important to note that size arguments are most effective in determining when two metals *can* form continuous solid solutions. They do not do well at predicting whether solid solutions *do* form and whether alloy systems without solid solutions segregate or form compounds.

III. RESULTS

A. General considerations

The results are presented in several stages. First, the general influence of the energy parameters is described at $x=\frac{1}{2}$ and $Z=8$ by comparing the energies in the limiting cases of SRO. The effect of the one-electron parameters is discussed taking $U_A=U_B=V=0$, but not allowing charge transfer in the segregated limit. Then the modifications caused by including self-consistency are described.

Second, the predicted trends are compared with experimental information on alkali-alkali— and noble-noble—metal alloys. Finally, we discuss the particular example of the Na-K alloy system in detail. This example illustrates general features of the concentration dependence of the model.

The zero of total energy is always taken as the energy of the segregated configuration at the same concentration. With this choice and $U_A = U_B$ the total energy and the magnitude of the charge transfer are invariant under the interchanges ($C \rightarrow -C$) or ($t_{AA} \leftrightarrow t_{BB}$ and $c_A \leftrightarrow c_B$). When $U_A \neq U_B$, the magnitude of the charge transfer and the total one-electron energy are invariant under these transformations; only the mean value of H_{ee} changes. The electronic charge transfer is always from the atom of larger E_{I0} to the one with smaller E_{I0}.

The unit of energy is defined to be $Z^{1/2}t$, where $t \equiv (t_{AA}t_{BB})^{1/2}$. The factor of $Z^{1/2}$ is included so that the results are relatively independent of the coordination number. In the model, the coordination number's main effect is to control the width of the bands. The second moment[12] of a pure metal LDOS with nearest-neighbor hopping t is Zt^2. Using $Z^{1/2}t$ as the unit energy compensates for the change in bandwidth with coordination number. It allows us to plot bcc and fcc alloys in the same graph.

B. One-electron parameters

The three independent one-electron parameters may be chosen to be $C/Z^{1/2}t$, $(t_{AA}/t_{BB})^{1/2}$, and t_{AB}/t. Figure 3 shows the regions in the ($C/Z^{1/2}t$, $(t_{AA}/t_{BB})^{1/2}$) parameter space where each of the three limiting types of SRO has the lowest energy for three different values of t_{AB}/t. The results are clearly understood as arising from two competing effects. As $C/Z^{1/2}t$ increases, there is more charge transfer and hybridization in the binary-ordered and random configurations and their energy decreases. The binary-ordered arrangement is most favored because a gap is created by the hybridization and only bonding states are filled. As $(t_{AA}/t_{BB})^{1/2}$ increases, the segregated configuration becomes favored because it has wider bands. The segregated configuration energy is proportional to the arithmetic mean of the elemental bandwidths; the random and binary-ordered configuration energies are roughly proportional to t_{AB}, which varies as the geometric mean of the elemental bandwidths. As $(t_{AA}/t_{BB})^{1/2}$ increases, the arithmetic mean becomes increasingly larger than the geometric mean. If one were to take $t_{AB} = \frac{1}{2}(t_{AA} + t_{BB})$, the binary-ordered compound would always be stable.

The balance between the binary-ordered, random, and segregated configuration energies changes with concentration. The binary-ordered configuration energy decreases sharply near $x = \frac{1}{2}$ as long-range order develops and a gap opens in the density of states. The random configuration energy is a smooth function of concentration. Near $x = \frac{1}{2}$ it always decreases with increasing concentration of the atom with the larger bandwidth. The concentration dependence is discussed in greater detail when we consider the example of the Na-K alloy system.

Following Pettifor,[2] we have attempted to model our results with an approximate density of states (DOS) consisting of one or two rectangular bands. The heights and widths of the rectangular bands are determined from the first three (zeroth, first, and second) moments of the true DOS.[12] Pettifor uses a single square band to model both the ran-

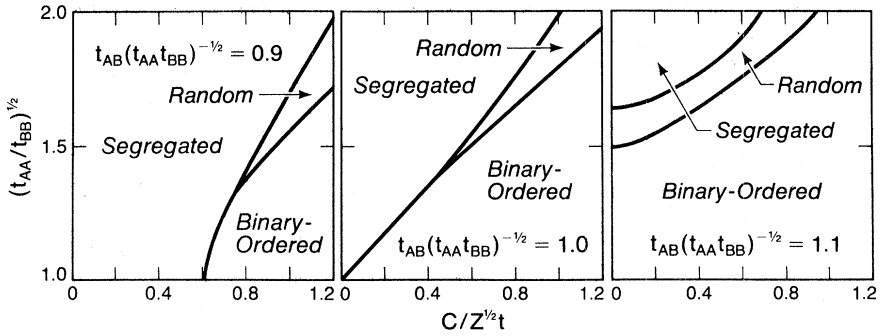

FIG. 3. Regions of relative stability of the segregated, random, and binary-ordered arrangements as a function of $C/Z^{1/2}t$ and $(t_{AA}/t_{BB})^{1/2}$ for three values of t_{AB}/t.

dom and binary-ordered DOS curves in his theory for the heats of formation of transition-metal compounds. The predictions of his model disagree with our results and with experiments on simple metals. The random arrangement is always favored in Pettifor's model unless $t_{AB}/t < 1$, and its total energy changes in the wrong direction as a function of concentration. Our results for the random configuration energy are qualitatively reproduced if two rectangular bands are used to model the DOS, one associated with the LDOS of each component. For example, the line where the random and segregated configuration energies are equal is reproduced within $\sim 5\%$ over the range plotted in Fig. 3. The binary-ordered configuration energy is more difficult to model because of the sharp features in the DOS associated with the formation of a gap.

C. Coulomb interactions

The effect of the on-site Coulomb interaction is straightforward and well understood. Nonzero values of U_A and U_B lead to a self-consistent on-site energy difference which is smaller than C. Thus the energies of the random and binary-ordered configurations increase and the amounts of charge transfer decrease. The segregated arrangement becomes more favored. In the graphs of Fig. 3 the area corresponding to segregated alloys increases as U_A and U_B increase.[32]

The intersite Coulomb interaction $V\alpha(\sigma)\Delta_I$ is treated better here than in previous calculations. Its importance is most clearly seen in a plot of energy versus SRO (Fig. 4). When $V=0$ the energy approaches the wrong limit as $\sigma \rightarrow +1$. Even small values of V produce the correct asymptotic behavior in this limit. This is only because we have used a form for $\alpha(\sigma)$ which approaches ∞ at $\sigma = +1$ as the exact $\alpha(\sigma)$ must.

For larger values of V, the binary-ordered configuration energy begins to change drastically. These values are unphysical. When $U + 2V\alpha(\sigma) < 0$ the effective on-site energy decreases as more electrons are added. If $U_i + 2V\alpha(-1) < -|t_{ii}|$ the pure metal is unstable against charge-density waves.

D. Comparison with real alloys

Figure 5 shows the region in which each limiting type of SRO has the lowest energy for $t_{AB}/t = 1$,

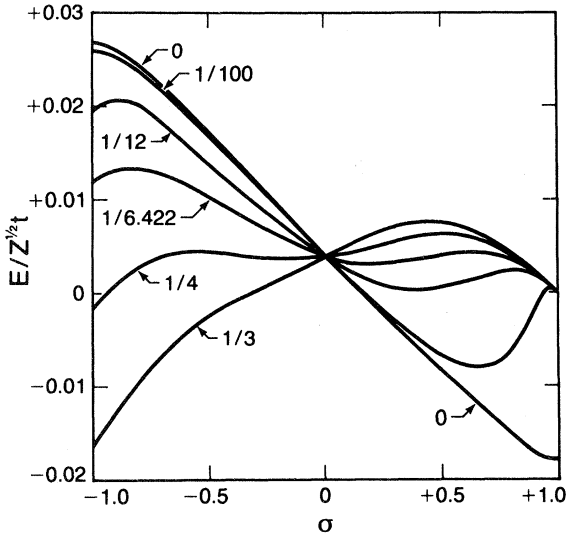

FIG. 4. Total energy of the alloy as a function of short-range order for various values of V. The other parameters are $Z=8$, $x=\frac{1}{2}$, $U_A=U_B=1.12Z^{1/2}t$, $t_{AB}=t$, $(t_{AA}/t_{BB})^{1/2}=1.5$, and $C=0.606Z^{1/2}t$.

$U=U_A=U_B=1.12Z^{1/2}t$, and $V=U/(6.422)$. For the same parameters, Fig. 6 gives the magnitude of the charge transfer associated with a given value of $C/Z^{1/2}t$ for $t_{AA}=t_{BB}$. The binary-ordered charge transfer is unaffected by $(t_{AA}/t_{BB})^{1/2}$ because only $A-B$ bonds occur. The charge transfer in the ran-

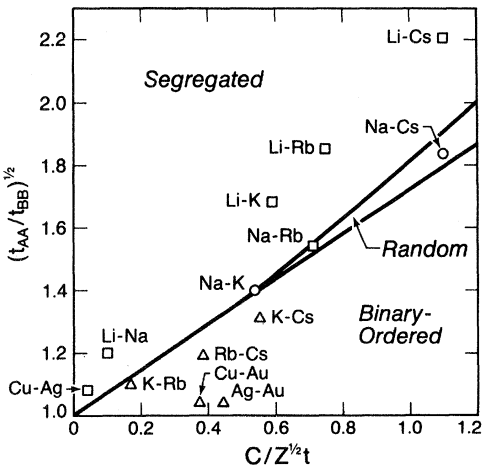

FIG. 5. Regions of stability as a function of $C/Z^{1/2}t$ and $(t_{AA}/t_{BB})^{1/2}$ for $t_{AB}=t$, $x=\frac{1}{2}$, $Z=8$, $U_A=U_B=6.422V=1.12Z^{1/2}t$. Values for real monovalent alloy systems are plotted: Squares indicate systems that segregate at all concentrations; circles indicate systems that form A_2B compounds but no solid solutions; triangles indicate systems with extended regions of solid solubilities and in some cases binary-ordered compounds.

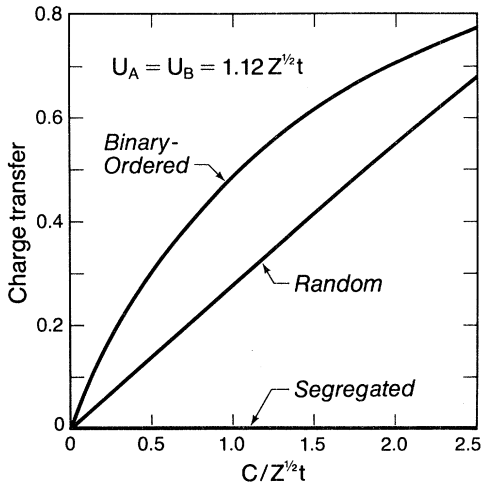

FIG. 6. Magnitude of the charge transfer (electrons/atom) as a function of $C/Z^{1/2}t$ for $t_{AA}=t_{BB}=t_{AB}$, $x=\frac{1}{2}$, $Z=8$, $U_A=U_B=6.422V=1.12Z^{1/2}t$. Electron charge is transferred to the element with lowest E_{I0}, the on-site energy.

dom configuration decreases by about 10% as $(t_{AA}/t_{BB})^{1/2}$ varies from 1 to 2. Electronic charge is always transferred to the element with lowest E_{I0}.

Also plotted in Fig. 5 are points corresponding to each of the alkali-alkali— and noble-noble—metal alloy systems. Squares are used to indicate systems which segregate at all concentrations, circles indicate systems which form A_2B compounds but no solid solutions, and triangles indicate systems with extended ranges of solid solubility and in some cases compounds. The predicted binary-ordered and random energies and charge transfers are given in Table II. Even with our simple choice of parameters, the results of the model are in good qualitative agreement with experiment. No attempt has been made to improve the fit by varying the value of U. In the following paragraphs we discuss each group of alloys in detail.

The lithium alloys are all found to segregate, even in the liquid state.[33] The Li-Na system has a miscibility gap with a critical point at 715 K. The other lithium alloys have immiscibility critical temperatures which are too high to have been measured ($T>1300$ K). Our model predicts that all four should segregate, and is consistent with a much lower critical temperature in Li-Na than in the other three alloys. The asymmetry with concentration in the immiscibility gap of Li-Na is in

TABLE II. Calculated energies and charge transfers at $x=\frac{1}{2}$.

Alloy ($A-B$)	Energy[a] Random (meV/atom)	Energy[a] Binary-ordered (meV/atom)	Charge transfer[b] Random (electrons/atom)	Charge transfer[b] Binary-ordered (electrons/atom)
Li-Na	+12.2	+29.9	+0.0279	+0.0826
Li-K	+43.8	+110.6	+0.1510	+0.3430
Li-Rb	+49.7	+131.6	+0.1853	+0.4051
Li-Cs	+53.7	+155.9	+0.2522	+0.5186
Na-K	+0.0	+2.0	+0.1449	+0.3208
Na-Rb	−1.3	+3.4	+0.1871	+0.3914
Na-Cs	−11.7	−2.8	+0.2720	+0.5172
K-Rb	−0.5	−2.0	+0.0472	+0.1286
K-Cs	−6.7	−15.6	+0.1506	+0.3267
Rb-Cs	−3.7	−9.8	+0.1065	+0.2493
Cu-Ag	+3.2	+4.6	+0.0111	+0.0144
Cu-Au	−38.9	−50.1	−0.1071	−0.1384
Ag-Au	−51.1	−65.9	−0.1270	−0.1641

[a]The segregating energy is always taken to be zero.
[b]A positive number indicates electron-charge transfer from B to A in the A-B pair of column 1.

the direction predicted by the model.

Near room temperature, the alloy systems K-Rb, K-Cs, and Rb-Cs form continuous solid solutions at all concentrations.[33] Recent experiments[34] show that the compound K_2Cs forms, but only below 185 K. No compounds have yet been observed in K-Rb or Rb-Cs. The model predicts that all three should form a binary compound at $T=0$. However, the ordering energies are so small that the ordered phases would not be observed at room temperature. The largest predicted ordering energy is for K-Cs, the only system in which a compound is observed.

Unfortunately, the small cluster size and the Bethe-lattice topology did not allow us to examine the possibility of formation of A_2B compounds. However, the asymmetries with concentration that are discussed below suggest that a K_2Cs compound should be more stable than either a KCs or KCs_2 compound.

The predictions for the above alloy systems are relatively insensitive to changes in the energy parameters. For example, changing U by 15% changes the energies by only $1-10\%$. In contrast, the predictions for the alloy systems Na-K, Na-Rb, and Na-Cs are altered drastically by this change in U. This is because they lie in the random configuration region of Fig. 5 where the energy balance between arrangements is changing.

Experiments on Na-K, Na-Rb, and Na-Cs show that the solid metals are only slightly soluble in each other. The compounds Na_2K and Na_2Cs are found[33] to form at 280 K and 265 K. No Na_2Rb compound has been observed,[33] which is surprising since Rb is intermediate in all respects between K and Cs. The reaction forming Na_2Cs is very sluggish and lower-temperature work on Na_2Rb might reveal such a compound. The model's predictions at $x=\frac{1}{2}$ are not in agreement with experimental observations. This discrepancy may occur because the value of U we chose was $\sim 15\%$ too large, because of size effects, or because we could not include the possibility of an A_2B compound. We discuss the last possibility later.

The predicted values for the energies[35] of noble-noble—metal alloys all have the correct sign.[31] In contrast, a previous calculation[16] using the extended CBLM, predicted all three alloys would form ordered compounds. This calculation was in error because an unphysically large value for $V\alpha(-\frac{1}{3})$ was used. A large value of $V\alpha(-\frac{1}{3})$ favors charge transfer and thus a binary-ordered structure. For the value used previously, the pure materials are in fact unstable against charge-density waves. With reasonable values for $V\alpha(-\frac{1}{3})$, the signs of the ordering energies are very insensitive to the choice of parameters. The alloys lie far from the binary-ordered—to—segregated transition in Fig. 5.

Experimentally, the alloy Cu-Ag is found to segregate in the solid phase.[31,33] There is no miscibility gap in the liquid phase, but anomalous behavior observed in thermodynamic quantities may be evidence of substantial SRO. Measurements of ΔH suggest a random energy of about 40 meV/atom. Our predicted value is substantially lower. The discrepancy may be due to the difference in the atomic radii of Cu and Ag, which should make the appropriate value of t_{AB} less than t. It may also be related to the d bands, which are not included in our calculation.

Both Cu-Au and Ag-Au exhibit complete solid solubility at sufficiently high temperatures.[31,33] The compound CuAu forms below 683 K and Cu_3Au and $CuAu_3$ form[6] below 663 and 473 K. Thermodynamic measurements[33] indicate incipient compounds with compositions AgAu, Ag_3Au, Ag_3Au_2, and $AgAu_3$, but no long-range ordering is found in x-ray experiments. Considerable short-range order is present in AgAu below 800 K.

The random and binary-ordered energies of CuAu are measured to be -52.9 and -96.7 meV/atom, respectively.[31] The predicted values are -38.9 and -50.1 meV/atom. The model gives a lower energy for Cu_3Au than for $CuAu_3$, in agreement with experiment. As noted earlier, no structure with $\sigma=-1$ is possible on an fcc lattice. However, it is interesting to note that for $\sigma=-1$ the CBLM gives an energy of -94.3 meV/atom which is remarkably close to the observed energy of the Cu-Au ordered compound. The calculated energy for $\sigma=-\frac{1}{3}$ might be closer to the experimental value if the effect of LRO were included correctly.

The random configuration energy of Ag-Au is measured at about -48 meV/atom. The exact value is difficult to determine because of residual SRO. The extended CBLM gives -51.1 meV/atom for the random energy and -65.9 meV/atom for the binary-ordered energy. It is interesting that although Ag-Au is predicted to have a lower binary-ordered energy than Cu-Au, more long-range order is present in the Cu-Au system. Elastic energies may be responsible for this apparent contradiction. The Ag and Au atoms are very close in size while Cu is 10% smaller.[36,37] Thus, elastic energies are larger in the Cu-Au alloy

system than in the Ag-Au alloy system. Elastic interactions are very long range and may be strong enough in Cu-Au to stabilize LRO, but too weak to have any effect in Ag-Au.

E. Detailed study of the Na-K alloy

To exhibit the concentration dependence of the model, we discuss the Na-K alloy system in detail. The random and binary-ordered configuration energies are plotted as functions of concentration in Fig. 7. The DOS and Fermi level are shown for various concentrations in Fig. 8.

The random energy is a smooth function of concentration. When $t_{AA}=t_{BB}$, the energy is symmetric about $x=\frac{1}{2}$. As $(t_{AA}/t_{BB})^{1/2}$ increases, the energy becomes increasingly asymmetric. Near $x=\frac{1}{2}$ the random energy always decreases with increasing concentration of the atom with the larger bandwidth. In the case of Na-K, the energy actually changes sign in this region.

The binary-ordered configuration energy decreases sharply near $x=\frac{1}{2}$. In this region a gap opens in the density of states for any nonzero value of C. At $c_{\mathrm{Na}}=\frac{1}{2}$, the Fermi level is in the center of the gap so that only bonding states are filled. As c_{Na} changes from $\frac{1}{2}$, the gap decreases and the

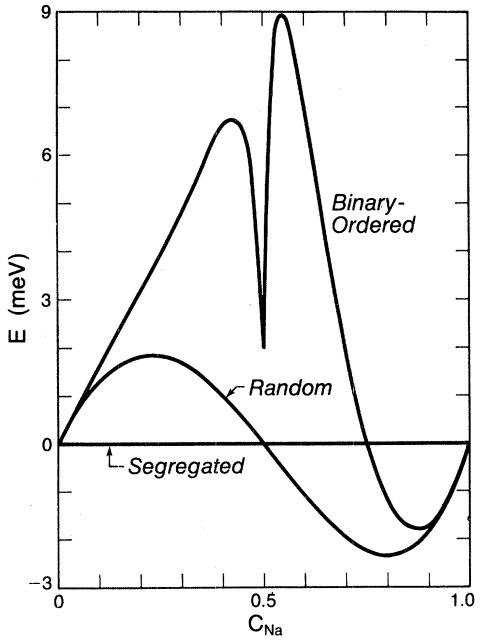

FIG. 7. Total energy of the random and binary-ordered arrangements relative to the segregated configuration for the Na-K system.

Fermi level moves away from it so that less energy is gained from hybridization. The gap decreases at different rates for $c_{\mathrm{Na}}<\frac{1}{2}$ and for $c_{\mathrm{Na}}>\frac{1}{2}$, as shown in Fig. 8. In the binary-ordered configura-

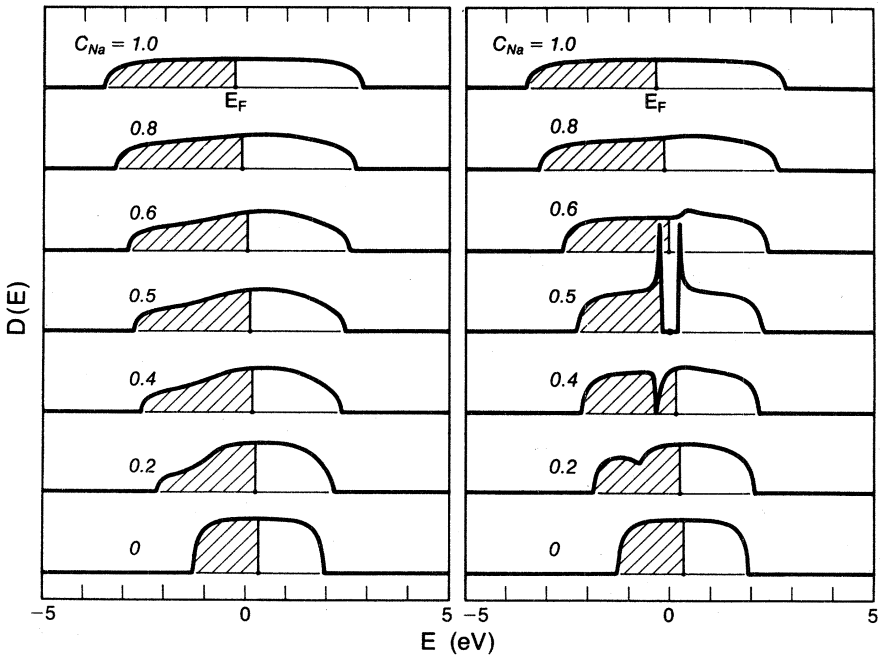

FIG. 8. Density of electronic states of the Na-K system in the random and binary-ordered configurations for various concentrations.

tion, only $A-B$ bonds and $I-I$ bonds between two atoms of the majority element exist. The gap in the DOS is bigger when the hopping parameter for the like-atom bonds is smaller. In Na-K, $t_{KK} < t_{NaNa}$ and thus the gap is larger for $c_{Na} < \frac{1}{2}$. Away from $c_{Na} = \frac{1}{2}$ the binary-ordered energy behaves smoothly, following the trends seen in the random energy.

The cluster of one atom and Bethe-lattice effective medium do not allow us to calculate the energy of an A_2B compound. However, it seems reasonable that the asymmetry in the random energy is mirrored in the energy of binary-ordered compounds. The energy of the binary-ordered configuration is significantly lower at $c_{Na} = \frac{2}{3}$ than at $c_{Na} = \frac{1}{3}$ and, with proper inclusion of the effect of LRO, might well approach the experimental value of -6.3 meV/atom in Na_2K.

IV. SUMMARY AND CONCLUSIONS

We have applied[16] the extended CBLM and a new technique for calculating the long-range effect of charge transfer to study the alkali-alkali— and noble-noble—metal alloy systems. As seen in Fig. 5, our results are in good qualitative agreement with experimental observations. We predict correctly that the alloys Li-Na, Li-K, Li-Rb, Li-Cs, and Ag-Cu segregate. Experimental values for the energies of random lithium alloys are not available but our predicted values have the right magnitude to explain the observed phase diagrams. Our value for the energy of Ag-Cu is too small. The alloys K-Rb, K-Cs, and Rb-Cs are predicted to form compounds, but with very low ordering energies. The largest calculated ordering energy is that of KCs. All three alloys form continuous solid solutions at room temperature. The only compound that has been reported is K_2Cs, and it does not form above 185 K. The alloys Ag-Au and Cu-Au are also predicted to form ordered compounds. Experiments indicate that compounds with several compositions form in both systems. The predicted values of the random energies of these alloys are within 10—30% of experiment. The remaining alloys Na-K, Na-Rb, and Na-Cs are all predicted to form random alloys. In fact, Na-Rb is reported to segregate and the other alloys form the compounds Na_2K and Na_2Cs. In the present application of our model, the energy of an A_2B compound cannot be calculated. However, observed asymmetries with respect to concentration suggest that the energies of Na_2K and Na_2Cs would be lower than those of NaK and NaCs if they could be calculated. It is not understood why Na-Rb does not behave like the other two alloy systems.

Previous calculations[16] with the extended CBLM of the ordering energies of noble-noble—metal alloys, gave the wrong sign for the ordering energy of Cu-Ag. An unrealistic model for the Coulomb potential from surrounding atoms heavily favored the formation of binary-ordered compounds. The model gave particularly bad values for the Coulomb potential in alloys with a tendency to segregate. We have devised a method for summing the off-site Coulomb interaction for arbitrary concentration and short-range order. Using this method the error in the sign of the ordering energy of Cu-Ag was corrected, and reasonable calculations of the effects of charge transfer in segregated alloys were possible for the first time. Our treatment of the Coulomb sum is not limited to use in conjunction with the extended CBLM. It can be incorporated in any alloy formalism that includes SRO through pair probabilities and gives a projected LDOS for each type of atom. However, in its present form, the technique is only applicable to studies of varying SRO on a fixed lattice.

Further investigation along the lines presented here could follow several directions:

(1) A larger cluster size. This improvement will test the convergence of the extended CBLM and allow a variety of different ordered compounds to be considered. It will also give information about the effect of fluctuations in the local environment on the LDOS and charge at a site.

(2) More basis orbitals at each site. A larger local basis would allow calculations on transition-metal alloys. These alloys are of more practical interest and are better described by a tight-binding Hamiltonian, which is the starting point for the CBLM.

(3) Detailed thermodynamic studies. As mentioned in the Introduction, calculations of the energy as a function of SRO can be combined with Kikuchi's formalism for the entropy[7] to give free energies and phase diagrams.

(4) Inclusion of self-consistent changes in the hopping parameters with both charge transfer and interatomic spacing. The latter step would allow the elastic energy to be included in the model, but requires an accurate theory of the variation in atomic spacing with concentration and SRO.

ACKNOWLEDGMENTS

This work was supported in part by the NSF through Grant No. DMR8106494. One of the authors (M.O.R.) gratefully acknowledges support of an IBM Predoctoral Fellowship.

APPENDIX

To calculate $\bar{\phi}_I$, Eq. (9), we divide the sum over $\vec{R}_l$ into contributions from shells of constant n, the smallest number of nearest-neighbor bonds connecting $\vec{R}_l$ to the origin. We write

$$\bar{\phi}_I = V \sum_n q_n \sum_J g_{IJ}(n)\Delta_J \ , \tag{A1}$$

where the q_n are purely geometric coefficients obtained by summing $R/|\vec{R}_l|$ over all $\vec{R}_l$ with the same value of n.

From the recursion relation for $g_{IJ}(n)$, Eq. (10), we may write

$$\sum_J \Delta_J g_{IJ}(n+1) = \sum_J \Delta_J \sum_K g_{IK}(n)\frac{y_{JK}}{c_K} = \sum_K \gamma_K g_{IK}(n) \ , \tag{A2}$$

where

$$\gamma_K \equiv \sum_J \Delta_J \frac{y_{JK}}{c_K} = \Delta_K \frac{y_{KK}}{c_K} + \Delta_\kappa \frac{y_{\kappa K}}{c_K} \ ,$$

and κ is used to indicate the opposite type of atom from K. Charge conservation, Eq. (8), implies

$$\gamma_K = \Delta_K \left[\frac{y_{KK}}{c_K} - \frac{y_{\kappa K}}{c_\kappa} \right] , \tag{A3}$$

and the formulas for the pair probabilities, Eq. (2), give

$$\gamma_K = \Delta_K[(c_K + c_\kappa\sigma) - c_K(1-\sigma)] = \sigma\Delta_K \ . \tag{A4}$$

Thus, we obtain

$$\sum_J g_{IJ}(n+1)\Delta_J = \sigma \sum_J g_{IK}(n)\Delta_K \ , \tag{A5}$$

and

$$\bar{\phi}_I = V\Delta_I \alpha(\sigma) \ , \tag{A6}$$

where

$$\alpha(\sigma) = \sum_n q_n \sigma^n \ . \tag{A7}$$

The first ten coefficients, q_n, for bcc and simple cubic lattices are given in Table III. As $|\sigma|$ approaches 1 distant shells become more and more important. Fortunately one only needs to calculate q_n for a few shells because they quickly approach an asymptotic limit. For large n, the number of sites on a shell goes as n^2 and $|\vec{r}_i - \vec{r}_j|$ goes as n so that q_n is proportional to n, i.e., $q_n \to \rho n$. Also given in Table III is the deviation of each coefficient from the asymptotic value. We rewrite the sum as

TABLE III. Coefficients of the power series defining $\alpha(\sigma)$.

	bcc lattice (CsCl)			simple cubic lattice (NaCl)	
n	q_n	$q_n - \rho n$	n	q_n	$q_n - \rho n$
1	8	−0.2448	1	6	+0.2172
2	16.5446	+0.0550	2	11.4853	−0.0803
3	24.7369	+0.0024	3	17.3519	+0.0035
4	32.9810	+0.0016	4	23.1301	−0.0012
5	41.2249	+0.000 86	5	28.9135	−0.000 54
6	49.4694	+0.000 43	6	34.6966	−0.000 31
7	57.7141	+0.000 37	7	40.4795	−0.000 20
8	65.9588	+0.000 28	8	46.2624	−0.000 13
9	74.2036	+0.000 12	9	52.0452	−0.000 09
10	82.4484	+0.000 09	10	57.8281	−0.000 07
	$\rho = 8.244\,83$			$\rho = 5.782\,81$	
Madelung constant = −1.7627[a]			Madelung constant = −1.7476[a]		

[a]Agrees to all significant digits with other published values.

$$\alpha(\sigma)=\sum_n \rho n\sigma^n+\sum_n (q_n-\rho n)\sigma^n$$
$$=\rho\sigma/(1-\sigma)^2+\sum_n (q_n-\rho n)\sigma^n . \quad \text{(A8)}$$

The first term is exactly summable and the remainder is a rapidly converging power series for all σ.

An *ad hoc* approximation for $\alpha(\sigma)$ can be obtained from only the coordination number, Z, and the Madelung constant, $\alpha(-1)$. The coordination number gives q_1 and the other coefficients can be approximated by an asymptotic form which is fitted to the Madelung constant. One writes

$$\alpha(\sigma)\approx\rho'\sigma/(1-\sigma)^2+(Z-\rho')\sigma ,$$
$$\alpha(-1)=3\rho'/4-Z , \quad \text{(A9)}$$

which yield

$$\rho'=4[\alpha(-1)+Z]/3 . \quad \text{(A10)}$$

The resulting function is within 1% of the exact formula for the two examples given above.

It should be noted that the approach used here is only applicable to lattices which can be divided into two interpenetrating sublattices such that all nearest neighbors of an atom on one sublattice belong to the other sublattice. This condition excludes close-packed lattices such as fcc and any other lattice which contains odd-numbered rings of nearest-neighbor bonds. In such systems the pair probabilities are insufficient for specifying the SRO. It may be possible to extend the current approach to these lattices by incorporating higher-order cluster probabilities. For segregating SRO, the simple model for $\alpha(\sigma)$ should give good results on any lattice with a choice of $\alpha(-1)$ near -2. The peculiar topologies which are important in ordered compounds are not relevant to segregated alloys.

[1]A. R. Miedema, P. F. de Châtel, and F. R. de Boer, Physica (Utrecht) 100B, 1 (1980), and references therein.

[2]D. G. Pettifor, Phys. Rev. Lett. 42, 846 (1979); Solid State Commun. 28, 621 (1978).

[3]A. R. Williams, C. D. Gelatt, Jr., and V. L. Moruzzi, Phys. Rev. Lett. 44, 429 (1980).

[4]R. E. Watson and L. H. Bennett, Phys. Rev. Lett. 43, 1130 (1979).

[5]M. Schlüter and C. M. Varma, Bull. Am. Phys. Soc. 26, 300 (1981).

[6]See, for instance, C. Barrett and T. B. Massalski, *Structure of Metals,* 3rd ed. (McGraw-Hill, New York, 1966), pp. 275–305.

[7]R. Kikuchi, Phys. Rev. 81, 988 (1951).

[8]J. Friedel, Nuovo Cimento Suppl. 7, 287 (1958).

[9]R. H. Parmenter, Phys. Rev. 97, 587 (1955).

[10]J. L. Beeby, Phys. Rev. 135, A130 (1964).

[11]P. Soven, Phys. Rev. 156, 809 (1967); H. Ehrenreich and L. M. Schwartz, in *Solid State Physics,* edited by H. Ehrenreich, F. Seitz, and D. Turnbull (Academic, New York, 1976), Vol. 31, p. 149.

[12]M. Cyrot and F. Cyrot-Lackman, J. Phys. F 6, 2257 (1976).

[13]R. Haydock, in *Solid State Physics,* edited by H. Ehrenreich, F. Seitz, and D. Turnbull (Academic, New York, 1980), Vol. 35, p. 216, and references therein.

[14]H. W. Diehl and P. L. Leath, Phys. Rev. B 19, 587 (1976); 19, 596 (1976); F. Brouers and F. DuCastelle, J. Phys. F 5, 45 (1975); A. Gonis and J. W. Garland, Phys. Rev. B 18, 3999 (1978).

[15]F. Yndurain and L. M. Falicov, Solid State Commun. 17, 1545 (1975); L. M. Falicov and F. Yndurain, Phys. Rev. B 12, 5664 (1975).

[16]R. C. Kittler and L. M. Falicov, J. Phys. C 9, 4259 (1976); Phys. Rev. B 18, 2506 (1978); 19, 527 (1978).

[17]For a description of a Bethe lattice (Cayley tree), see C. Domb, Adv. Phys. 9, 145 (1960); especially pp. 283–4 and 297. See also A. Cayley, *Collected Mathematical Papers* (Cambridge University Press, Cambridge, 1889–98) Vol. 13, p. 26.

[18]J. M. Cowley, Phys. Rev. 77, 669 (1950).

[19]V. Heine, in *Solid State Physics,* edited by H. Ehrenreich, F. Seitz, and D. Turnbull (Academic, New York, 1980), Vol. 35, p. 1, and references therein.

[20]J. Rudnick and E. A. Stern, Phys. Rev. B 7, 5062 (1973).

[21]The last two approximations become exact in the limit of large distances and are susceptible to local corrections.

[22]D. DeFontaine, in *Solid State Physics,* edited by H. Ehrenreich, F. Seitz, and D. Turnbull (Academic, New York, 1979), Vol. 34, p. 73; P. C. Clapp, Phys. Rev. B 4, 255 (1971).

[23]Every $\vec{R}_l$ is associated with a unique value of n.

[24]Self-consistent variations in t_{ij} with various parameters (chemical shifts, charge transfer, etc.), which depend on x and σ can be included in a straightforward manner. This would require several additional parameters which might obscure the underlying physics. We chose not to include these effects.

[25]The model is not applicable to alkali-noble—metal alloys because the pure metals have different crystal structures.

[26]C. E. Moore, *Atomic Energy Levels* (U. S. Government Printing Office, Washington, D.C.), Vol. I (1949), Vol. II (1971), and Vol. III (1958).

[27]F. S. Ham, Phys. Rev. 128, 82 (1962).

[28]G. A. Burdick, Phys. Rev. 129, 138 (1963).

[29]N. E. Christensen, Phys. Status Solidi B 54, 551 (1972).

[30]N. E. Christensen and B. O. Seraphin, Phys. Rev. B 4, 3321 (1971).

[31]R. Hultgren, R. L. Orr, P. D. Anderson, and K. K. Kelley, *Selected Values of Thermodynamic Properties of Metals and Alloys* (Wiley, New York, 1963).

[32]For $U_A \neq U_B$ and small values of C the total energy may actually decrease as U_A and U_B decrease. There is a linear term in the electron-electron energy proportional to $U_A - U_B$ which decreases the total energy when the atom with the lowest on-site energy has the smallest U_I.

[33]M. Hansen, *Constitution of Binary Alloys* (McGraw-Hill, New York, 1958); R. P. Elliot, *Constitution of Binary Alloys, First Supplement* (McGraw-Hill, New York, 1965); F. A. Shunk, *Constitution of Binary Alloys, Second Supplement* (McGraw-Hill, New York, 1969).

[34]U. Shmueli, V. Steinberg, T. Sverbilova, and A. Voronel, J. Phys. Chem. Solids 42, 19 (1981); V. Steinberg, T. Sverbilova, and A. Voronel, *ibid.* 42, 23 (1981).

[35]It should be noted that the noble-noble—metal alloys are plotted in the same graph with the alkali-alkali—metal alloys. With our choice of abscissa, $C/Z^{1/2}t$, the results are independent of coordination number within plotting accuracy.

[36]C. Kittel, *Introduction to Solid State Physics,* 5th ed. (Wiley, New York, 1976), p. 31.

[37]It is interesting to note that both Au-Cu and Ag-Cu have size differences of $\sim 10\%$, yet the first system forms several compounds, and the second segregates. Size alone obviously cannot explain ordering trends.